gels

MDPI

Article

Gum Arabic Modulates Redox–Ionic Microenvironments via Rheology and Kinetics to Induce Selective Cytotoxicity in Colorectal Cancer Cells

Emre Cebeci [1], Büşra Yüksel [1], Reyhan Aliusta [2], Şahin Yılmaz [1], Ertuğrul Osman Bursalıoğlu [3], Mustafa Eray Bozyel [4], Halise Betül Gökçe [5], Şaban Kalay [6], Şükran Özdatlı Kurtuluş [7], Ahmet Arif Kurt [8,9], Fikrettin Şahin [1] and Ismail Aslan [4,10,11,*]

1 Department of Genetics and Bioengineering, Faculty of Engineering, Yeditepe University, Kayışdağı, Istanbul 34755, Türkiye; emrecebeci34@gmail.com (E.C.); busra.yuksel@yeditepe.edu.tr (B.Y.); sahin.yilmaz@yeditepe.edu.tr (Ş.Y.); fsahin@yeditepe.edu.tr (F.Ş.)
2 Venar Sağlık A. S., Başkent Organized Industrial Zone, Teknokent Blvd. No:39, Malıköy, Sincan, Ankara 06909, Türkiye; reyhaneser@hotmail.com
3 Department of Medical Services and Techniques, Vocational School of Health Services, Sinop University, Sinop 57000, Türkiye; ebursalioglu@sinop.edu.tr
4 SFA R&D Private Health Services Co., Ltd., Teknopark Blv, No:1 3A Z01, Teknopark Istanbul, Pendik, Istanbul 34890, Türkiye; m.eraybozyel@gmail.com
5 Department of Pharmaceutical Technology, Faculty of Pharmacy, Afyonkarahisar Health Sciences University, Afyonkarahisar 03030, Türkiye; betul.aslan@afsu.edu.tr
6 Division of Biochemistry, Department of Basic Pharmaceutical Sciences, Faculty of Pharmacy, University of Health Sciences, Istanbul 34668, Türkiye; saban.kalay@sbu.edu.tr
7 Department of Pharmaceutical Toxicology, Faculty of Pharmacy, University of Health Sciences, Istanbul 34668, Türkiye; sukranozdatli.kurtulus@sbu.edu.tr
8 Department of Pharmaceutical Technology, Faculty of Pharmacy, Suleyman Demirel University, Isparta 32000, Türkiye; ahmetkurt@sdu.edu.tr
9 Polisome R&D Pharmaceutical Industry Trade Company, Isparta 32000, Türkiye
10 ATABIO Technologies Co., Ltd., Teknopol İstanbul, Istanbul 34903, Türkiye
11 Department of Pharmaceutical Technology, Hamidiye Faculty of Pharmacy, University of Health Sciences, Istanbul 34668, Türkiye
* Correspondence: ismail.aslan@sbu.edu.tr; Tel.: +90-216-504-81-82

Abstract

Background: Gum Arabic (GA) is a natural polysaccharide widely recognized for its antioxidant and anti-inflammatory properties; however, its functional behavior as a biopolymeric gel and the mechanisms underlying its selective effects on cancer-related redox microenvironments remain insufficiently characterized. It is imperative to note that the interaction between its physicochemical properties and its biological activity in colorectal cancer remains to be fully clarified. Methods: This study aimed to evaluate the antineoplastic potential of GA in human colorectal cancer (CRC) cell lines (HT-29 and HCT-116) compared to normal fibroblasts (MRC-5) using the MTS assay. Oxidative stress-related molecular responses were assessed by quantitative PCR analysis of GPX4, GSTA2, CAT, NFKB, and SOD1 expression. In parallel, extracellular concentrations of key metal ions (Fe^{2+}, Zn^{2+}, Mn^{2+}, Mg^{2+}, Cu^{2+}, and Al^{3+}) were quantified following GA exposure. To establish its functional gel characteristics, rheological measurements were performed to assess viscosity and shear-dependent behavior, and USP-compliant in vitro kinetic studies were conducted to evaluate time-dependent release properties. Results: GA induced dose-dependent cytotoxicity in HT-29 and HCT-116 colorectal cancer cells, while MRC-5 fibroblasts exhibited comparatively higher viability across the tested concentration range, indicating reduced sensitivity in normal cells. Rheological analysis revealed concentration- and ion-dependent viscoelastic behavior, identifying a 10% (*w*/*w*) GA formulation as optimal due to its balanced low-shear viscosity and controlled shear-thinning properties. Kinetic studies

Academic Editors: Alejandro Sosnik and Jilong Wang

Received: 24 December 2025
Revised: 17 January 2026
Accepted: 29 January 2026
Published: 3 February 2026

demonstrated a defined, diffusion-governed release profile under physiologically relevant conditions. At the molecular level, significant upregulation of GPX4 and GSTA2 was observed in both cancer cell lines, whereas NFKB expression increased selectively in HT-29 cells, with no notable changes in CAT or SOD1 expression. Additionally, GA treatment resulted in marked increases in Fe^{2+}, Zn^{2+}, and Mn^{2+} levels, indicating modulation of the redox–ionic microenvironment. Conclusions: These findings demonstrate that GA functions as a natural, ion-responsive biopolymeric system with defined rheological and kinetic properties, capable of selectively targeting colorectal cancer cells through coordinated genetic and ionic regulation of oxidative stress. Collectively, the results position GA as a promising functional gel-based platform for future redox-modulated therapeutic strategies in colorectal cancer.

Keywords: Gum Arabic; functional gels; rheology; kinetic behavior; redox modulation; colorectal cancer

1. Introduction

In recent years, an annual increase in the number of colorectal cancer cases has been observed. It is the third leading cause of cancer-related deaths worldwide and the fourth most commonly diagnosed cancer type [1,2]. According to the Global Cancer Statistics 2022 report, over 1.9 million new CRC cases and nearly one million deaths were reported globally [3]. These figures underscore the significant impact of CRC on public health and the urgent need for more effective, safe, and specific therapeutic strategies. Despite notable advances in surgery, chemotherapy, and targeted agents, treatment outcomes remain limited due to tumor heterogeneity, non-specific cytotoxicity to healthy tissues, and the emergence of drug resistance [4,5]. Molecularly, CRC is characterized by chromosomal instability (CIN), microsatellite instability (MSI), and epigenetic modifications such as the CpG island methylator phenotype (CIMP), all of which contribute to variability in therapeutic response [6]. Analyses of pathway and gene interactions conducted at the systems level indicate that colorectal cancer progresses through common oncogenic networks. These networks are therefore considered to be targetable for novel therapeutic approaches [7].

Standard chemotherapeutics including 5-fluorouracil, irinotecan, and oxaliplatin, although widely used, are often associated with dose-limiting toxicities and off-target effects, which can significantly impair patients' quality of life [8]. In this context, the capacity of nutrition-based and postbiotic-rich natural components to demonstrate antitumour effects in colorectal cancer cells provides substantial rationale for the development of more selective and safer treatment strategies [9]. Additionally, mutations in genes like KRAS and BRAF contribute to drug resistance, making treatment outcomes less predictable and reinforcing the need for novel, more selective therapeutic options [8].

As a result, attention has increasingly shifted towards bioactive compounds derived from natural sources, particularly those with known antioxidant, anti-inflammatory, and anticancer properties [10–12]. Natural substances often act through multi-targeted pathways and present fewer side effects compared to conventional agents, thus making them promising candidates for integrative oncology approaches [13]. Among these, plant-derived polysaccharides have emerged as significant due to their capacity to modulate oxidative stress, immunity, and cellular metabolism [14,15]. In a study conducted by Teixeira and colleagues in 2025, a pyrimidine-based compound (PP) was shown to be a promising anticancer agent against colorectal cancer; and it was reported that albumin/hyaluronic acid gel nanoparticles with a biopolymer gel structure exhibited potent anticancer activity by carrying this compound [16]. In 2022, Khaing and colleagues demonstrated the efficacy of an imatinib mesylate-loaded

resin/cinnamon oil-based in situ gel, based on a biopolymer gel, against colorectal cancer cells [17]. This system was thus defined as a potential and sustainable drug carrier for chemotherapy. Based on its gel-forming and ion-binding properties, we hypothesized that Gum Arabic may function as an ion-responsive gel-like system capable of modulating the extracellular ionic microenvironment. Through regulation of metal ion availability, GA may selectively influence redox homeostasis in colorectal cancer cells.

Gum Arabic (GA) is a natural, gummy exudate predominantly obtained from the umbrella-shaped branches of *Acacia seyal* and *Acacia senegal*, primarily cultivated in Sudan, Chad, and Nigeria [18,19]. Structurally, GA consists mainly of an arabinogalactan-protein complex and serves as a rich source of dietary fiber enriched with essential minerals such as calcium (Ca^{2+}), magnesium (Mg^{2+}), and potassium (K^{+}) [20,21]. This distinctive biochemical composition not only supports its conventional use as a stabilizing agent in the food industry but also underpins its emerging pharmacological importance due to a wide array of bio-functional properties It is becoming increasingly evident that GA has significant anti-inflammatory, antioxidant, gut-supporting, and anticancer properties. This renders it a promising candidate for various therapeutic applications, especially in cancer treatment [22–26]. Recent findings also suggest that GA may modulate redox signaling and oxidative stress responses—mechanisms intricately linked to colorectal tumorigenesis [22]. However, despite these promising observations, there is still a lack of comprehensive molecular-level investigations assessing the selectivity and mechanistic pathways of GA in colorectal cancer models.

A study synthesized GA, which contains multiple aldehyde groups, and developed smart hydrogels for the purpose of delivering nanocurcumin. The hydrogels in question demonstrated notable levels of toxicity towards breast cancer cells, with the release of the material being pH-responsive [27]. The development of hybrid nanogels containing GA and albumin has enabled the effective delivery of the drug 5-fluorouracil. It has been reported that these nanogels have the capacity to inhibit the growth of cancer cells by increasing the release of drugs in acidic environments [28]. In one particular study, GA was utilized as a stabilizing agent in the fabrication of various transition metal dichalcogenide (TMD) nanolayers. It has been documented that these developed structures have the capacity to effectively destroy breast cancer cells by exhibiting photothermal effects under laser light [29].

A study was conducted to increase the bioavailability of curcumin. This study resulted in the production of GA aldehyde-gelatin nanogels. The nanogels in question are successfully absorbed by breast cancer cells, thereby enabling controlled drug release and treatment [30]. The present study investigates the synthesis of Nisin-loaded sodium alginate-GA nanoparticles to combat colon cancer. The system in question has been shown to trigger apoptosis (programmed cell death) in cancerous cells by protecting against pH changes in the digestive system. In the study conducted by Soans et al. (2025) [31], GA nanoparticles were utilized to enhance the stability of Gallic acid. The investigation focused on the antioxidant properties of these nanoparticles and their potential impact on the stability of Gallic acid. These particles demonstrated a selective response, particularly against liver and breast cancer cells. As posited by Hassani et al. (2020) [32], a system was devised for the controlled release of doxorubicin, employing gelatin and GA processed on graphene oxide nano-sheets. This triple nanocomposite achieves high drug release in cancer cells without harming normal lung cells. As stated by Hassani et al. (2020) [33], the antioxidant capacity of curcumin nanoparticles prepared using GA and sodium alginate was measured. The study demonstrated that this system was particularly efficacious in the inhibition of human liver cancer cells (HepG2) [33].

Thiolation was employed as a method of enhancing the mechanical strength and adhesion properties of acacia gum. This newly developed material demonstrated the capacity to suppress cervical cancer cells by more than 60%, while exhibiting no adverse effects on normal cells [34]. In this study, zinc oxide nanoparticles were synthesized using *Acacia nilotica*, more commonly known as the *Acacia* tree, bark. The efficacy of these particles was found to exceed that of conventional extracts in the treatment of liver cancer, diabetes, and oxidative stress. As posited by Azeem et al. (2024) [35], a novel nanocomposite comprising GA, silver, and copper oxide has been synthesized. The material exhibited a lethal effect against breast and liver cancer cells while also displaying strong antimicrobial properties against various pathogenic microorganisms. As posited by Hashem et al. (2025) [36], the immunomodulatory effects of gold nanoparticles synthesized using *Yucca filamentosa* and GA were investigated. It was hypothesized that these particles could open a new avenue in the treatment of prostate and breast cancer by targeting tumor-supporting cells [37]. Gold nanoparticles were produced using an environmentally friendly method with GA and cinnamon. It was asserted that these nanoparticles induced a high level of viability loss in colon cancer cells (HCT-116), even at very low doses [38].

A study was conducted in which rhenium disulfide layers, stabilized with GA, were coated with silver nanoparticles. The application of heat, generated by a laser, destroys breast cancer cells through the creation of oxygen radicals and the utilization of a photothermal effect [39]. An investigation was undertaken to ascertain the impact of nanocomposites comprising GA, curcumin, and selenium on colon cancer. These bio-based compounds have been demonstrated to induce severe DNA damage and apoptosis in cancer cells. As posited by Al-Duais et al. (2025) [40], the utilization of silica particles loaded with thymochinone, coated with GA, constitutes a treatment modality for brain tumors (glioma). The core–shell structure of the nanoparticle ensured greater release of the drug in the acidic tumor environment and protection of healthy nerve cells. As posited by Shahein et al. (2019) [41], a series of silver-zinc oxide hybrid nanocomposite membranes was produced, with a basis in cellulose acetate and GA. The incorporation of silver into the material has been demonstrated to enhance its thermal stability and efficacy in combating breast cancer and microbial infections [42]. The present study investigates the use of zein nanoparticles stabilized with GA, with a view to increasing the solubility of cancer drugs (TKIs). This formulation resulted in a twofold increase in the drug's absorption by cells and a corresponding increase in the rate of cancer cell death [43].

In a study on targeted drug delivery, a novel targeted delivery system for piperine (Pip), an alkaloid derived from black pepper, was developed. Piperine, a constituent of black pepper, was targeted using GA-coated hydroxyapatite particles. The present study demonstrated that the system, when modified with folic acid, was capable of successfully inhibiting colon cancer cells without causing harm to normal cells. AbouAitah et al. (2020) [44] synthesized GA nanocomposites containing copper and zinc oxide nanoparticles using a green method. The efficacy of these composites was demonstrated in vitro against a range of cancer cells and a variety of bacteria and fungi at safe doses. In the study conducted by El-Sayyad et al. (2025) [45], the efficacy of resveratrol in cancer treatment was enhanced through the utilization of gold nanoparticles and Arabic gum. The study demonstrated that GA enhanced the bioavailability of resveratrol against breast, pancreatic, and prostate cancer by increasing the loading of resveratrol onto the nanoparticle surface [46]. Iron oxide nanocomposites modified with GA and PEG were synthesized. These magnetic structures have been shown to trigger cell death by inducing genetic changes in prostate cancer cells [47].

This study investigates the anticancer potential of GA in two CRC cell lines (HT-29 and HCT-116) compared to healthy human fibroblasts (MRC-5). The cytotoxic effects were

evaluated via MTS assay, and gene expression analyses were conducted to assess antioxidant response. In addition, changes in extracellular metal ion concentrations were measured to explore GA's possible involvement in redox regulation through ionic pathways. By integrating these assessments, this study aims to provide novel insights into the selective action of GA in cancer cells and its potential application as a natural therapeutic agent in CRC.

2. Results and Discussion

2.1. Cytotoxic Effect of Gum Arabic

The cytotoxic effect of Gum Arabic (GA) was evaluated in colorectal cancer and normal cell lines using the MTS assay. HCT-116 and HT-29 colorectal cancer cell lines, along with the MRC-5 normal human lung fibroblast line, were exposed to a range of GA concentrations (2.5% to 50% w/v) for 72 h. The administration of GA resulted in a decline in cell viability that was proportional to the administered dose, in both cancer cell lines. Notably, HT-29 cells showed a more pronounced sensitivity to GA compared to HCT-116, as demonstrated by a sharper decline in viability at lower concentrations (Figure 1a,b).

In contrast, MRC-5 fibroblasts retained higher viability particularly at concentrations $\leq$10% (w/v), consistent with their higher IC_{50} value compared with CRC cell lines (Figure 1c). These results indicate that CRC cell lines display higher sensitivity to GA compared with MRC-5 fibroblasts, as reflected by lower IC_{50} values in malignant cells (Figure 1c). The half-maximal inhibitory concentrations (IC_{50}) were estimated based on cell viability curves and are summarized in Table 1. The IC_{50} for HCT-116 cells was calculated to be approximately 10%, while that of HT-29 cells ranged between 5% and 10%, confirming their higher susceptibility. For MRC-5 cells, the IC_{50} value was broader, between 10% and 20%, further suggesting reduced toxicity in normal cells.

These findings support the hypothesis that Gum Arabic may exhibit selective anticancer activity, warranting further investigation into its molecular mechanism and potential therapeutic application.

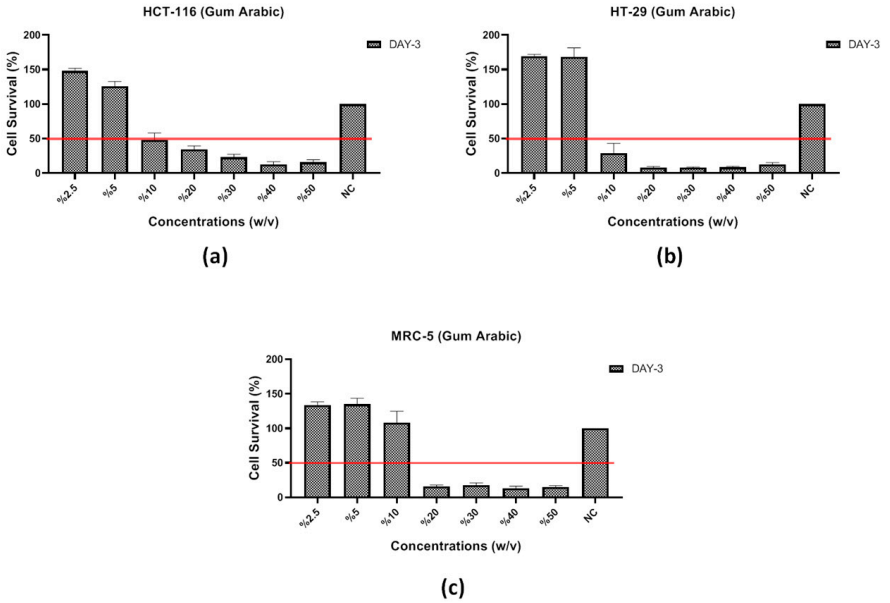

Figure 1. MTS assay results showing the cell survival rates (%) of (**a**) HCT-116 and (**b**) HT-29 colorectal cancer cell lines, and (**c**) MRC-5 normal fibroblast cells after 72 h of GA exposure at varying concentrations (w/v). Cell viability is presented as the percentage of viable cells relative to the negative control (NC).

Table 1. IC_{50} Values of treatment for cell lines.

Treatments	IC_{50} Value of HCT-116 (*w*/*v*)	IC_{50} Value of HT-29 (*w*/*v*)	IC_{50} Value of MRC-5 (*w*/*v*)
Gum Arabic (GA)	10%	7.5%	15%

In order to assess the cellular response to GA treatment, the expression levels of antioxidant-related genes along with the concentrations of extracellular metal ions were analyzed in HCT-116 and HT-29 colorectal cancer cell lines (Figure 2a,b). GA exposure resulted in a marked upregulation of GPX4 and NFKB expression levels in both HCT-116 and HT-29 cell lines compared to the negative control (**** $p < 0.0001$). While the expression levels of CAT and SOD1 remained unchanged in HCT-116 cells, a significant elevation of SOD1 expression was observed in HT-29 cells ($p < 0.01$), suggesting a cell line-specific antioxidant response. GST2A expression, however, showed no significant change in either of the cell lines.

To further elucidate the extracellular biochemical alterations induced by GA, metal ion concentrations (Mg^{24}, Mg^{25}, K^{39}, K^{41}, Ca^{43}, and Ca^{44}) in the culture media of HCT-116 and HT-29 cells were measured after 72 h of exposure (Figure 3a,b). A substantial increase in the concentrations of magnesium (both Mg^{24} and Mg^{25}), potassium (K^{39} and K^{41}), and calcium isotopes (Ca^{43} and Ca^{44}) was observed in GA-treated groups compared to the negative control in both cell lines (**** $p < 0.0001$). This elevation indicates a potential disruption in ion homeostasis and highlights the involvement of GA in modulating extracellular mineral dynamics.

Following GA treatment, the concentrations of selected heavy metal ions—namely Al^{27}, Mn^{55}, Zn^{65}, and Zn^{67}—in the extracellular medium were significantly increased in both HT-29 and HCT-116 cell lines compared to their respective controls (Figure 4a,b). Among these, Zn isotopes showed the most prominent elevation (**** $p < 0.0001$), suggesting a possible alteration in zinc homeostasis. Interestingly, Al^{27} levels did not significantly change in HT-29 cells, whereas a slight but statistically insignificant increase was observed in HCT-116 cells (ns). These findings might reflect a GA-induced modulation of metal ion transport or cellular detoxification processes.

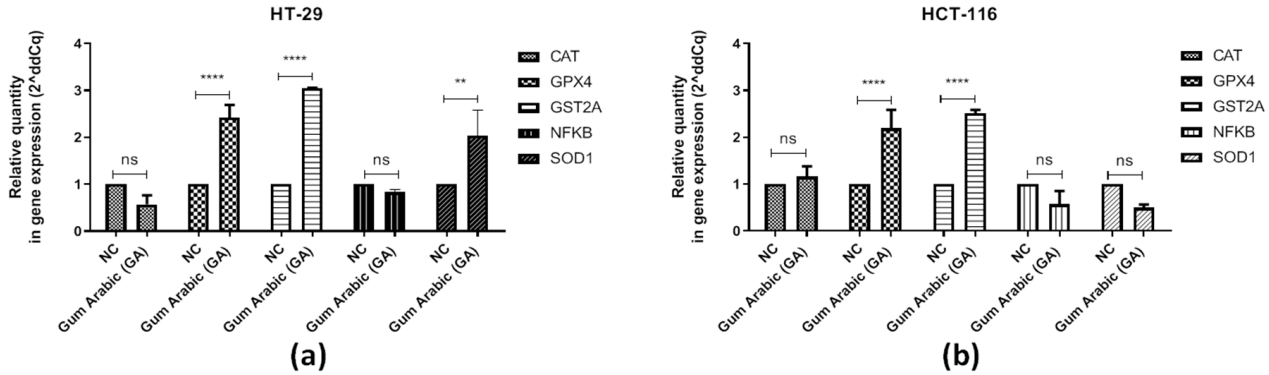

Figure 2. Relative mRNA expression levels of antioxidant-related genes in (**a**) HT-29 cancer cell line (**b**) HCT-116 cancer cell line after 72 h of GA exposure. (ns: not significant, ** $p < 0.01$, **** $p < 0.0001$).

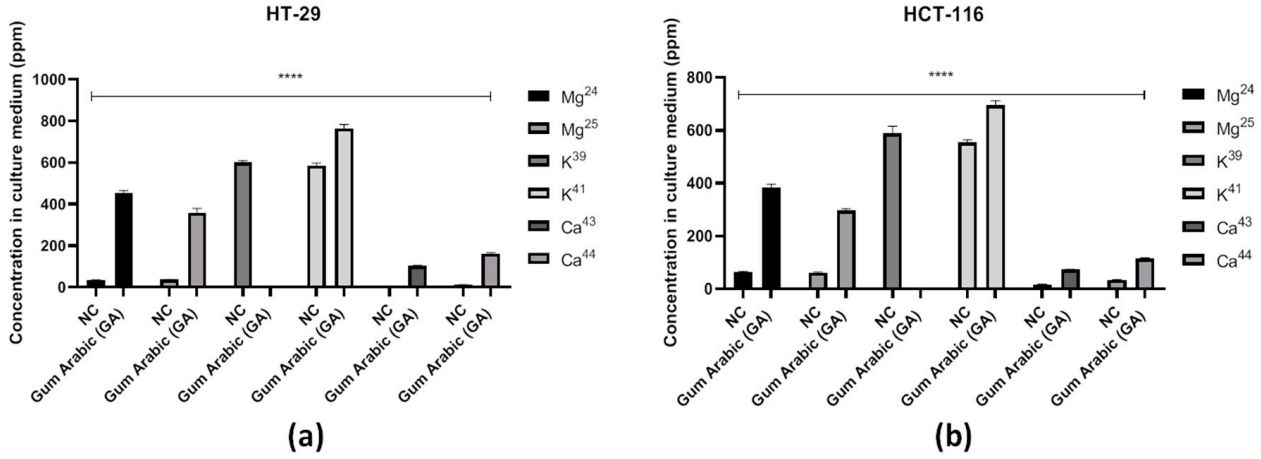

Figure 3. Concentrations of selected metal ions (Mg^{24}, Mg^{25}, K^{39}, K^{41}, Ca^{43}, and Ca^{44}) in the culture medium of (**a**) HT-29 and (**b**) HCT-116 CRC cell lines after 72 h of Gum Arabic (GA) treatment. Metal ion levels were determined using ICP-MS. The following abbreviations are used to indicate statistical significance: ns: not significant, **** $p < 0.0001$.

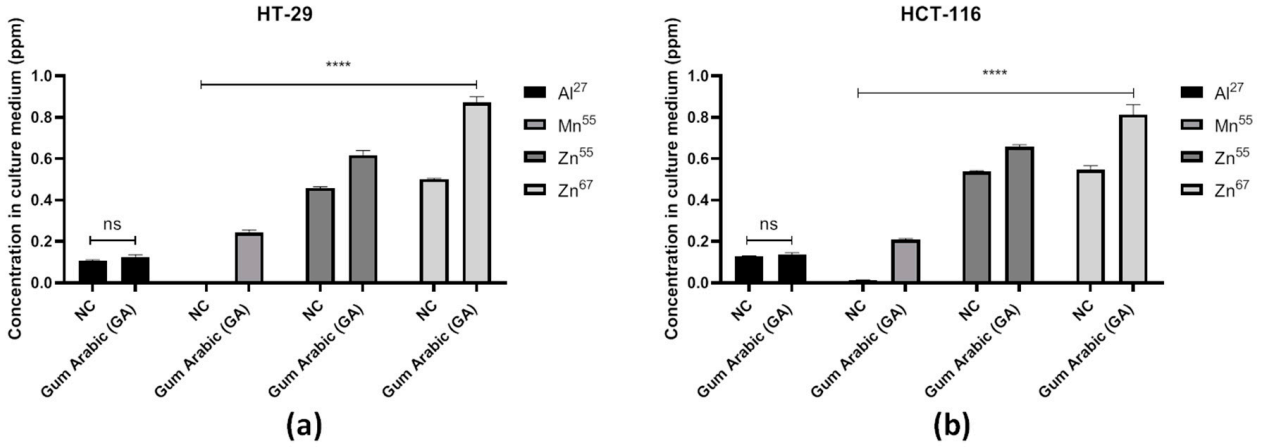

Figure 4. Concentrations of selected trace elements (Al^{27}, Mn^{55}, Zn^{65}, and Zn^{67}) in the culture medium of (**a**) HT-29 and (**b**) HCT-116 CRC cell lines after 72 h Gum Arabic (GA) treatment. The levels of trace elements were quantified using ICP-MS. Metal ion levels were determined using ICP-MS. The following abbreviations are used to indicate statistical significance: ns: not significant, **** $p < 0.0001$.

2.2. In Vitro pH-Dependent Release and Kinetic Behavior of Gum Arabic Matrix

The in vitro cumulative drug release profiles of the GA-based formulation under simulated gastrointestinal conditions are presented in Figure 5. Release behavior was strongly dependent on the pH of the dissolution medium. At pH 1.2 (gastric phase), cumulative drug release remained minimal throughout the 24 h study period, reaching approximately 10% at the final sampling point. The release profile showed a slow and nearly linear increase with time, indicating effective suppression of drug release under acidic conditions. In the pH 6.8 (intestinal phase), a moderate increase in cumulative release was observed. Drug release progressed gradually over time, reaching approximately 55–60% after 24 h. Compared with the gastric phase, the intestinal medium resulted in a noticeably higher release rate, while complete drug liberation was not achieved. In contrast, the pH 7.4 (colonic phase) exhibited a pronounced and time-dependent increase in cumulative drug release. An initial increase was observed within the first few hours, followed by a sustained release pattern, reaching approximately 85–90% at 24 h. The colonic phase consistently showed the highest cumulative release values across all time points.

Overall, the release profiles demonstrated a clear pH-dependent behavior, with cumulative release increasing in the order pH 1.2 < pH 6.8 < pH 7.4, as summarized in Figure 5. All data are presented as mean values obtained from three independent measurements (n = 3).

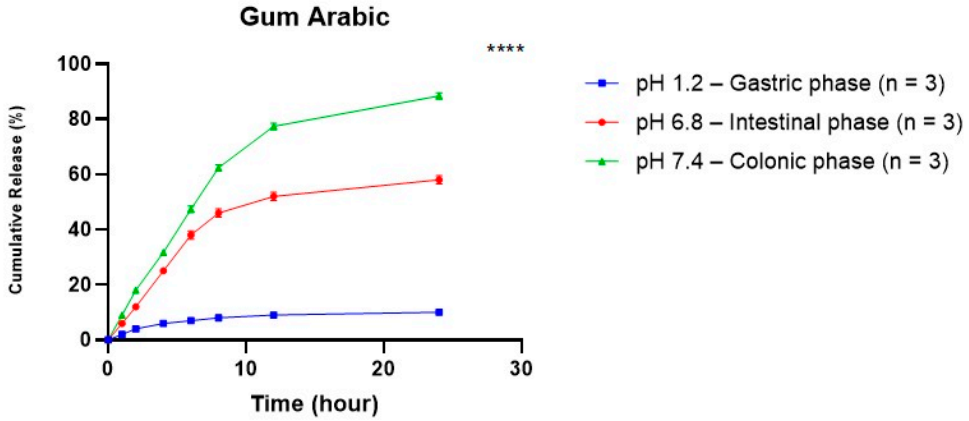

Figure 5. In vitro cumulative drug release profiles of the Gum Arabic-based formulation under simulated gastrointestinal conditions. Release studies were performed sequentially at pH 1.2 (gastric phase), pH 6.8 (intestinal phase), and pH 7.4 (colonic phase) at 37 ± 0.5 °C. Data represent mean ± SD (n = 3). The formulation exhibited minimal drug release under acidic conditions, moderate release at intestinal pH, and a pronounced, sustained release in the colonic phase, indicating pH-dependent release behavior. The following abbreviation is used to indicate statistical significance: **** $p < 0.0001$.

2.3. Kinetic Model Analysis

It is important to note that the kinetic experiments conducted in this study did not involve a loaded anticancer drug or model compound. The analysis was conceived to characterise the pH-dependent release and diffusion behaviour of GA itself as a functional biopolymeric matrix. The Higuchi model showed a good linear fit, suggesting diffusion-controlled release behavior. The Korsmeyer–Peppas model provided an excellent correlation (R^2 = 0.993), with the release exponent n = 0.67, indicating anomalous (non-Fickian) transport, governed by a combination of diffusion and polymer relaxation mechanisms (Table 2).

Table 2. Kinetic parameters of drug release from Gum Arabic-based formulation (pH 7.4).

Model	Equation	Parameter	Value	R^2
Higuchi	($M_t = k_H, t^{1/2}$)	(k_H) (%·$h^{-1/2}$)	17.9	0.981
Korsmeyer–Peppas	($M_t/M_{infty} = k, t^n$)	(k) (h^{-n})	0.46	0.993
		(n)	0.67	

In vitro cumulative drug release studies were performed using a USP-compliant dissolution method under sink conditions. Dissolution experiments were conducted at 37 ± 0.5 °C using a paddle apparatus (USP Apparatus II) containing 900 mL of release medium and operated at a constant agitation speed. To simulate gastrointestinal transit, samples were exposed to sequential pH conditions, consisting of pH 1.2 (simulated gastric fluid) for the initial 2 h, followed by pH 6.8 (simulated intestinal fluid) and subsequently pH 7.4 (simulated colonic fluid), with the dissolution medium adjusted stepwise at predetermined time points [48,49].

At specific intervals, aliquots (V_s, mL) were withdrawn, filtered, and analyzed for drug content by UV–Vis spectrophotometry or HPLC using a previously constructed calibration curve. An equal volume of fresh, pre-warmed medium was immediately replaced to

maintain constant volume and sink conditions. The cumulative amount of drug released at time t (M_t) was calculated with correction for sample replacement according to:

$$M_t = C_t V + \sum_{i=1}^{t-1} C_i V_s$$

where C_t is the drug concentration at time t, V is the total dissolution volume, and V_s is the sample volume withdrawn.

Cumulative drug release was expressed as a percentage of the initially loaded drug amount (M_0) using the equation:

$$\%\text{Cumulative release} = \frac{M_t}{M_0} \times 100$$

Release profiles were further analyzed by fitting the experimental data to commonly used kinetic models, including the Higuchi model and the Korsmeyer–Peppas power law model, with the first ~60% of release data used for mechanism evaluation where applicable [50–52].

The apparent viscosity of GA aqueous solutions was strongly influenced by both polymer concentration and shear rate at 37 °C. At low concentrations (1–5% *w*/*w*), viscosity values remained low throughout the tested shear rate range and exhibited only minor reductions with increasing shear rate, indicating weak shear-thinning behavior and near-Newtonian flow characteristics at higher shear rates.

GA solutions at 10% (*w*/*w*) displayed a clear and reproducible shear-thinning behavior, characterized by higher apparent viscosity at low shear rates followed by a progressive decrease as the shear rate increased. This concentration provided a balanced rheological profile, maintaining sufficient viscosity at low shear rates while allowing efficient flow under higher shear conditions.

At higher concentrations (15–20% *w*/*w*), a marked increase in low-shear viscosity was observed, accompanied by a more pronounced shear-thinning response. However, the viscosity–shear rate curves at these concentrations showed a steeper decline and greater sensitivity to shear compared with the 10% (*w*/*w*) system.

Across all samples, apparent viscosity values converged at higher shear rates, suggesting reduced dependence on shear under these conditions. Overall, among the tested concentrations, the 10% (*w*/*w*) GA solution exhibited the most favorable combination of moderate viscosity and controlled shear-thinning behavior under the applied measurement conditions.

GA, a natural exudate derived from acacia species, was approved as a safe food additive by the US Food and Drug Administration (FDA) in 1969 [53]. From a chemical perspective, the substance is categorized as a complex, water-soluble dietary fiber, comprising primarily arabinogalactan-protein complexes [54,55]. Beyond its nutritional role, GA has a long history of use in traditional medicine and continues to be widely used in the food, pharmaceutical, and cosmetic industries for its emulsifying, stabilizing, and bioactive properties [54,56]. In recent years, scientific interest in the therapeutic potential of GA has increased due to its remarkable anti-obesity [57], antioxidant [58], antimicrobial [59], immunomodulatory [60], and anticancer activities [29].

In view of these encouraging properties, the present study sought to examine the possible anticancer effects of GA in colorectal cancer models. In order to achieve this objective, in vitro experiments were performed using HCT-116 and HT-29 colorectal cancer cell lines. The cytotoxic effects of GA were evaluated by MTS assays, and the expression levels of antioxidant-related genes (GPX4, CAT, SOD1, GSTA2, and NFKB) were analyzed by qPCR after 72 h of treatment. Furthermore, the extracellular concentrations of significant

metal ions, including magnesium (Mg^{2+}), calcium (Ca^{2+}), potassium (K^{+}), and zinc (Zn^{2+}), were measured using inductively coupled plasma mass spectrometry (ICP-MS), thereby offering additional insights into the ionic changes associated with GA exposure. In this context, the objective of the assays was to examine the effects of GA on cell viability, antioxidant response, and mineral balance in colorectal cancer cells.

In the present study, the administration of GA resulted in a concentration-dependent decline in cell viability, observed in both the HT-29 and HCT-116 colorectal cancer cell lines. It is noteworthy that HT-29 cells demonstrated a heightened sensitivity to GA, while the MRC-5 fibroblast cell line exhibited comparatively higher viability within the same concentration range. However, it should be emphasized that the non-malignant comparison in this study was limited to human fibroblasts. Consequently, it is imperative that these findings are interpreted as preliminary evidence of selective toxicity rather than definitive tissue-specific targeting. Further studies employing normal human colon epithelial cell models are required to fully validate colorectal tissue selectivity.

In this study, the effect of GA on cell viability was first evaluated in colorectal cancer cell lines (HCT-116 and HT-29) and a normal human fibroblast cell line (MRC-5). The results of the MTS assay demonstrated a dose-dependent decline in viability in both cancer cell lines following 72 h of GA exposure. A notable finding was the observation that HT-29 cells exhibited a heightened sensitivity to GA treatment in comparison to HCT-116 cells. Conversely, MRC-5 cells demonstrated higher levels of viability within the same concentration range, suggesting a selective cytotoxic effect of GA on malignant cells. These results suggest that GA exerts selective toxicity against colorectal cancer cells while sparing normal fibroblasts, supporting its potential as a safe anticancer agent. This observation is consistent with earlier findings concerning plant-derived polysaccharides, which have been shown to exhibit selective toxicity, selectively targeting cancer cells while exerting minimal effects on normal cells [61].

In order to further investigate the cellular antioxidant response induced by Gum Arabic (GA), the expression levels of key genes associated with oxidative stress were evaluated, namely GPX4, GSTA2, CAT, NFKB, and SOD1. Firstly, SOD1, CAT, and GPX4 act in concert as essential components of the cellular antioxidant defense system: SOD1 has been shown to convert superoxide radicals into hydrogen peroxide, which is then detoxified by CAT and GPX4, thus preventing oxidative cell damage [62]. Additionally, GSTA2 plays a role in glutathione metabolism and contributes to cellular defense mechanisms against oxidative stress induced by reactive oxygen species (ROS) [63]. Furthermore, NFKB has been reported to contribute to cellular protection during oxidative stress by limiting the accumulation of reactive oxygen species (ROS) and modulating redox-sensitive signaling pathways [64]. In the present study, GA treatment significantly upregulated GPX4, GSTA2, and NFKB expression in both HT-29 and HCT-116 cell lines, while CAT and SOD1 levels remained unchanged. These results suggest that GA selectively activates glutathione-dependent antioxidant pathways and stress-responsive signaling, rather than the classical hydrogen peroxide detoxification enzymes, as part of its cytoprotective mechanism. In this context, the observed increase in NFKB expression, particularly in HT-29 cells, is discussed as a context-dependent cellular stress or redox-associated response rather than as a direct indicator of anticancer activity. These findings reflect a selective transcriptional response to GA treatment rather than providing direct evidence for a specific cytoprotective mechanism.

In the present study, GA treatment significantly upregulated GPX4 and GSTA2 expression in both HT-29 and HCT-116 cell lines. The upregulation of the GPX4 and GSTA2 genes following the application of GA reflects the glutathione-dependent antioxidant and detoxification response developed in cells against GA exposure, rather than indicating

direct inhibition of ferroptosis. These gene expression changes indicate that cells have developed a compensatory adaptation mechanism against increased oxidative and metabolic stress. These findings may indicate that GA supports glutathione-dependent antioxidant responses. However, rather than implying a direct cytotoxic mechanism, the observed increase in GPX4 expression is interpreted as a potential compensatory or adaptive response to GA-induced oxidative or redox-related stress. Given the established role of GPX4 in redox homeostasis and ferroptosis regulation [48], any association with ferroptosis-related pathways remains speculative and should be interpreted with caution within the scope of the present study. By contrast, CAT and SOD1 expression levels remained unchanged, suggesting a selective transcriptional response to GA treatment rather than a generalized antioxidant activation. These findings may indicate that GA supports glutathione-dependent detoxification mechanisms and contributes to the attenuation of lipid peroxidation. This response could potentially be associated with reduced oxidative stress and the inhibition of ferroptosis-like pathways, which are tightly regulated by GPX4 activity and intracellular glutathione levels [65]. By contrast, CAT and SOD1 expression levels remained unchanged, suggesting that GA's antioxidative effect may act preferentially through the glutathione-dependent pathway rather than classical ROS-scavenging.

To gain further insight into the ionic microenvironment influenced by GA treatment, the concentrations of selected metal ions—including Fe^{2+}, Mg^{2+}, Zn^{2+}, Mn^{2+}, Cu^{2+}, and Al^{3+}—were measured in the culture media of GA-treated cells. Among the measured ions, Fe^{2+}, Mg^{2+}, Zn^{2+}, and Mn^{2+} levels increased following GA exposure in both HT-29 and HCT-116 cell lines. Conversely, the augmentation in Fe levels evident within the culture medium after GA treatment does not provide direct evidence that ferroptosis is actively induced. This finding may be related to the natural mineral content of GA, passive ion release due to cellular stress, or changes in the medium composition. Therefore, it has been considered only to have an indirect and speculative relationship with the ferroptosis mechanism. These changes may reflect alterations in the extracellular ionic environment or cellular stress-associated responses rather than direct evidence of regulated cell death pathways. Although redox-active iron has been implicated in ferroptosis-related processes [66], no functional markers of ferroptosis were assessed in this study, and therefore any such association remains speculative. Given that Zn^{2+} and Mn^{2+} serve as cofactors for antioxidant enzymes, the observed changes may reflect broader stress-adaptive or homeostatic responses rather than direct evidence of enhanced enzymatic activity [67]. On the other hand, Al^{3+} levels remained unchanged, indicating that GA does not affect the uptake of non-essential or potentially toxic metals under the tested conditions.

Based on the balance between sufficiently elevated low-shear viscosity and controlled shear-thinning behavior without excessive flow resistance, the 10% (w/w) Gum Arabic solution was identified as the optimal concentration under the applied measurement conditions (Figure 6). The findings of this study suggest that GA may influence cellular stress responses and redox-associated pathways in colorectal cancer cells, as reflected by changes in antioxidant gene expression and extracellular ion balance. These observations provide proof-of-concept evidence and highlight the need for cautious interpretation, while providing a basis for future exploratory studies.

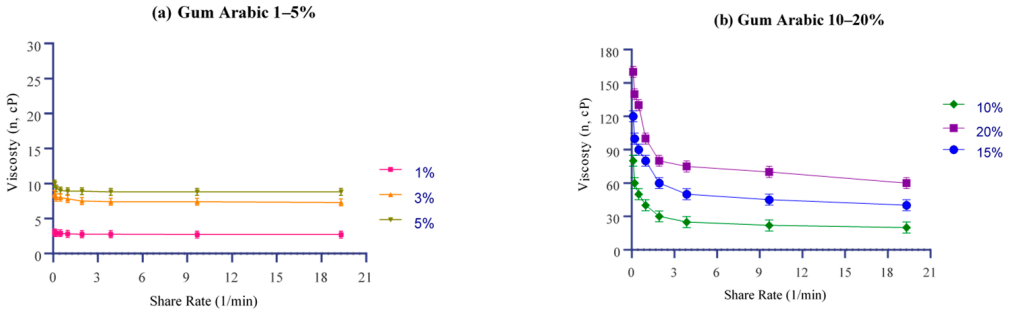

Figure 6. Rheological measurements of Gum Arabic in (**a**) 1, 3, and 5% concentrations and (**b**) 10, 15, and 20% concentrations.

3. Conclusions

This study provides original contributions to the existing literature by demonstrating the multifaceted physicochemical and biological effects of Gum Arabic (GA) in the context of colorectal cancer. Rheological evaluation revealed that GA exhibits concentration-dependent viscoelastic behavior, and based on the balance between sufficiently elevated low-shear viscosity and controlled shear-thinning behavior without excessive flow resistance, the 10% (*w*/*w*) GA solution was identified as the optimal concentration under the applied measurement conditions. This profile supports the functional gel-like nature of GA and its suitability for biomedical applications requiring both structural integrity and flow adaptability.

At the biological level, GA demonstrated marked and selective cytotoxicity in HT-29 and HCT-116 colorectal cancer cells while maintaining a non-toxic profile in healthy MRC-5 cells. The observed upregulation of GPX4 and GSTA2 suggests activation of glutathione-dependent antioxidant defense mechanisms, whereas alterations in NFKB expression indicate additional modulation of cellular stress response and redox regulation. Furthermore, the increased levels of Fe^{2+}, Zn^{2+}, and Mn^{2+} ions imply that GA influences redox homeostasis through modulation of the ionic microenvironment.

Taken together, these integrated rheological, ionic, and molecular findings indicate that GA functions as more than a passive natural polysaccharide, acting instead as a bioactive and ion-responsive system capable of targeting oxidative stress-related cancer mechanisms at both physicochemical and biological levels. Given its favorable rheological profile, low toxicity, and multilayered biological effects, GA emerges as a promising candidate for the future development of functional gel-based therapeutic strategies in colorectal cancer.

4. Materials and Methods

4.1. Cell Lines and Cell Culture Conditions

Human colorectal adenocarcinoma cell lines HCT-116 (CRL-247) and, HT-29 (HTB-38) along with the normal human lung fibroblast cell line MRC-5 (CRL-171), were obtained from the American Type Culture Collection (ATCC, Rockville, MD, USA). The HT-29 cells were maintained in Roswell Park Memorial Institute medium (RPMI-1640, #11875093, Gibco, ThermoFisher, Waltham, MA, USA), while the HCT-116 and MRC-5 cells were cultured in Dulbecco's Modified Eagle Medium (DMEM, #41966-029, Gibco). All culture media were enriched with 10% foetal bovine serum (FBS, #10500-064, Gibco) and 1% penicillin-streptomycin-amphotericin (PSA, Gibco). The cells were then subjected to an incubation process at a temperature of 37 °C, within a controlled environment containing 5% CO_2.

4.2. Cell Viability Assay

The cytotoxic effect of Gum Arabic (provided from Akavital, Ankara, Türkiye) was evaluated using the MTS assay [3-(4,5-dimethylthiazol-2-yl)-5-(3-carboxymethoxyphenyl)-

2-(4-sulfophenyl)-2H-tetrazolium salt] (#G3582, CellTiter 96® AQueous One Solution, Promega, Southampton, UK), following the manufacturer's protocol. The HT-29, HCT-116, and MRC-5 cells were seeded at a density of 5000 cells per well in 96-well flat-bottom plates and incubated at 37 °C in a humidified incubator containing 5% CO_2.

In biological experiments, GA was applied as a fully dissolved, simple aqueous solution in the culture medium, and no gel formation was observed under the experimental conditions. All GA solutions were freshly prepared and passed through a 0.22 μm pore-size sterile filter before cell treatment. Following the initial attachment stage, the cells were treated with GA at six different concentrations, ranging from 3000 μg/mL to 93.75 μg/mL. The cells were then incubated for a further 24, 48, and 72 h. At the end of the incubation period, the culture medium was carefully aspirated and replaced with an MTS solution (prepared in PBS containing 10% MTS reagent and 4.5 g/L D-glucose). Following a 90 min incubation period at a temperature of 37 °C, the absorbances were measured at a wavelength of 490 nm, employing an ELISA microplate reader (BioTek, Winooski, VT, USA). Cell viability was calculated as a percentage relative to the untreated control group for each cell line (HCT-116, HT-29, and MRC-5). The substance under discussion was not administered in a powder form; rather, it was administered in a liquid state. The stock solution was prepared by continuously agitating the GA powder in a sterile environment. Subsequently, a protracted hydration process was implemented to ensure complete dissolution and homogeneity. The obtained solutions were then subjected to filtration and sterilisation processes, and subsequently diluted to the desired concentrations prior to undergoing the cell treatment. Absorbance values were normalized to untreated negative control (NC) wells, defined as 100% viability. Experiments were performed in three independent biological replicates, each analyzed in technical triplicates. The results of the cell viability analysis were expressed as relative metabolic activity and normalized to the untreated control group (NC), which was defined as 100%. This was done so that values above 100% would reflect increased mitochondrial metabolic activity rather than absolute cell number.

4.3. Real-Time PCR

Total RNA was isolated using an RNA isolation kit (#740955.250, Machery-Nagel, Düren, Germany) according to the manufacturer's instructions. The concentrations of RNA were determined by measuring the light absorption of the samples at a wavelength of 260 nanometres using a spectrophotometer. Subsequently, cDNA was synthesised using the QuantiTect Reverse Transcription Kit (#205313, Qiagen, Hilden, Germany) in accordance with the manufacturer's protocols. RT-PCR was performed using SYBR Green (#4309155, Thermo Fisher, Waltham, MA, USA) and tested on three occasions using the iCycler RT-PCR detection system (Bio-Rad, Hercules, CA, USA). The housekeeping gene RPL30 was selected based on its stable expression across all experimental conditions.

The expression levels were normalized with respect to RPL30 (Ribosomal Protein L30) gene (F: 5′-ACAGCATGCGGAAAATACTAC-3′ R: 5′-AAAGGAAAATTTTGCAGGTTT-3′) levels. Genes and their corresponding primer sequences used in this study were as follows; SOD1 gene (F: 5′-GGCCTAGCGAGTTATGGCGA-3′ R: 5′-CCCAAGTCTCCAACATGCCTCT-3′), GPX4 gene (F: 5′-AAGTGGAACTTCACCAAGTTTGGAC-3′ R: 5′-GATTTTCGGGTCTGCCCCAC-3′), GSTA2 gene (F: 5′-AGACATAAAGGAGAGAGCCCTGATT-3′ R: 5′-TCACCTTCAGCAGAGGGAAGC-3′), CAT gene (F: 5′-CATGCAGGACAATCAGGGTGG-3′ R: 5′-CTCCCGTAGTCAGGGTGGAC-3′), NFKB1 gene (F: 5′-CCGCTTAGGAGGGAGAGCC-3′ R: 5′-AAGGTATGGGCCATCTGCTGT-3′).

4.4. Trace Element Analysis in Culture Medium

The elemental concentrations of Al^{27}, Mg^{24}, Mg^{25}, K^{39}, K^{41}, Ca^{43}, Ca^{44}, Mn^{55}, Zn^{55}, and Zn^{67} in the cell culture media were measured using an inductively coupled plasma mass spectrometry (ICP-MS, iCAP RQ, Thermo Scientific, Waltham, MA, USA). For sample preparation, 100 µL of culture supernatant was collected and diluted with ultrapure water to a final volume of 5 mL in acid-cleaned polypropylene tubes. The instrument was operated under optimized conditions with a nebulizer gas flow of 1.14 L/min, coolant gas flow of 14 L/min, auxiliary gas flow of 0.8 L/min, and a plasma power of 1051 W. Calibration was performed using certified standard solutions (Sigma Aldrich, Cat. No: 1.11355.0100) in multiple concentrations to ensure accurate quantification. Limits of detection (LOD) were determined based on calibration data, and all measured values were above the respective detection thresholds. Element concentrations were compared between treatment groups using identical analytical conditions.

4.5. Rheological Studies

Rheological measurements were performed on Gum Arabic aqueous solutions prepared at 1, 3, 5, 10, 15, and 20% (*w*/*w*) using deionized water without the addition of salts, sugars, alcohols, or polyols. Gum Arabic powder was gradually dispersed into water under continuous stirring to prevent agglomeration and allowed to fully hydrate for at least 12 h prior to measurements. Rheological characterization was carried out at 37 °C using a temperature-controlled rotational rheometer (Brookfield-type, Bruker, Bremen, Germany) operated in controlled shear rate (CSR) mode, following standardized rotational rheometry principles. The shear rate was increased stepwise from low to high values (expressed as 1/min, consistent with the graphical representation), and the apparent viscosity (cP) was recorded after steady-state conditions were achieved at each step. All measurements were performed in triplicate, and results are reported as mean values in accordance with ISO 3219-2:2021 [68] and ASTM D2196-18 [69], following established rheological principles described by Barnes, Hutton, and Walters (1989) [70].

4.6. Statistical Analysis

To account for multiple comparisons, post hoc correction was applied following one-way ANOVA using Dunnett's multiple comparisons test. Only adjusted *p*-values < 0.05 were considered statistically significant.

Author Contributions: Conceptualization, E.C., R.A., B.Y. and I.A.; methodology, E.C., B.Y., Ş.K., I.A. and F.Ş.; validation, E.C., B.Y., E.O.B. and I.A.; formal analysis, E.C., B.Y., Ş.Y. and Ş.Ö.K.; investigation, E.C. and B.Y.; data curation, E.C., B.Y., Ş.Y., Ş.Ö.K. and E.O.B.; writing—original draft preparation, E.C., B.Y., M.E.B. and I.A.; writing—review and editing, Ş.Y., M.E.B., H.B.G., A.A.K., E.O.B., Ş.K. and F.Ş.; visualization, E.C., B.Y. and M.E.B.; supervision, H.B.G., A.A.K., E.O.B. and Ş.K.; project administration, I.A. and F.Ş. All authors have read and agreed to the published version of the manuscript.

Funding: This research received no external funding.

Institutional Review Board Statement: Not applicable.

Informed Consent Statement: Not applicable.

Data Availability Statement: The data used to support the findings of this study are available from the corresponding author upon request.

Acknowledgments: The authors thank Akavital Company for providing Gum Arabic material support. The authors also acknowledge the use of ChatGPT 5.2 (OpenAI, San Francisco, CA, USA), which helped improve the English language, grammar, and overall clarity of the article. This tool did not contribute to data analysis, interpretation, or scientific conclusions. The authors have reviewed and edited the output and take full responsibility for the content of this publication.

Conflicts of Interest: Reyhan Aliusta was employed by the company Venar Sağlık A.S., Mustafa Eray Bozyel was employed by the company SFA R&D Private Health Services Co., Ltd., Ahmet Arif Kurt was employed by the company Polisome R&D Pharmaceutical Industry Trade Company and Ismail Aslan was employed by the company SFA R&D Private Health Services Co., Ltd. and ATABIO Technologies Co., Ltd. The remaining authors declare that the research was conducted in the absence of any commercial or financial relationships that could be construed as a potential conflict of interest.

Abbreviations

The following abbreviations are used in this manuscript:

GA	Gum Arabic
CRC	Colorectal Cancer
MTS	3-(4,5-dimethyl-thiazol-2)-5-(3-carboxy-methoxy-phenyl)-2-(4-sulfo-phenyl)-2H-tetrazolium salt
PFA	Paraformaldehyde
RPL30	Ribosomal Protein L30

References

1. Gao, Y.; Su, D.; Zhao, J.; Luo, Z.; Lin, X. Study on the Feasibility of Self-Assembling Peptides as a Three-Dimensional Culture Tool for Drug Screening of Colorectal Adenocarcinoma Cells. *Gels* **2025**, *11*, 394. [CrossRef]
2. Ozakpinar, O.B.; Dastan, H.; Gurboga, M.; Sayin, F.S.; Ozsavci, D.; Salihi, E.C. Carbon Nanofiber—Sodium Alginate Composite Aerogels Loaded with Vitamin D: The Cytotoxic and Apoptotic Effects on Colon Cancer Cells. *Gels* **2023**, *9*, 561. [CrossRef]
3. Bray, F.; Laversanne, M.; Sung, H.; Ferlay, J.; Siegel, R.L.; Soerjomataram, I.; Jemal, A. Global Cancer Statistics 2022: GLOBOCAN Estimates of Incidence and Mortality Worldwide for 36 Cancers in 185 Countries. *CA Cancer J. Clin.* **2024**, *74*, 229–263. [CrossRef]
4. Fadlallah, H.; El Masri, J.; Fakhereddine, H.; Youssef, J.; Chemaly, C.; Doughan, S.; Abou-Kheir, W. Colorectal Cancer: Recent Advances in Management and Treatment. *World J. Clin. Oncol.* **2024**, *15*, 1136–1156. [CrossRef]
5. Qi, X.; Dong, Y.; Wang, H.; Wang, C.; Li, F. Application of Turbiscan in the Homoaggregation and Heteroaggregation of Copper Nanoparticles. *Colloids Surf. A Physicochem. Eng. Asp.* **2017**, *535*, 96–104. [CrossRef]
6. Advani, S.M.; Advani, P.; DeSantis, S.M.; Brown, D.; VonVille, H.M.; Lam, M.; Loree, J.M.; Mehrvarz Sarshekeh, A.; Bressler, J.; Lopez, D.S.; et al. Clinical, Pathological, and Molecular Characteristics of CpG Island Methylator Phenotype in Colorectal Cancer: A Systematic Review and Meta-Analysis. *Transl. Oncol.* **2018**, *11*, 1188–1201. [CrossRef]
7. Bursalıoğlu, E.; Kalay, Ş.; Metin, S. Evaluation of Gene Interaction and Similarity in 17 Different Cancer Pathways. *J. Res. Pharm.* **2025**, *29*, 742–750. [CrossRef]
8. Zoetemelk, M.; Ramzy, G.M.; Rausch, M.; Nowak-Sliwinska, P.; Zoetemelk, M.; Ramzy, G.M.; Rausch, M.; Nowak-Sliwinska, P. Drug-Drug Interactions of Irinotecan, 5-Fluorouracil, Folinic Acid and Oxaliplatin and Its Activity in Colorectal Carcinoma Treatment. *Molecules* **2020**, *25*, 2614. [CrossRef] [PubMed]
9. Çelebi, L.T.; Bursalioglu, E.O.; Çakici, B.; Genel, N.; Kalbisen, H.T.; Aslan, I. Can Buttermilk (Ayran) with Its Postbiotic Content Be Used in the Protection of Colon Health? *J. Immunol. Clin. Microbiol.* **2025**, *9*, 127–137. [CrossRef]
10. Newman, D.J.; Cragg, G.M. Natural Products as Sources of New Drugs over the Nearly Four Decades from 01/1981 to 09/2019. *J. Nat. Prod.* **2020**, *83*, 770–803. [CrossRef] [PubMed]
11. Mungwari, C.P.; King'ondu, C.K.; Sigauke, P.; Obadele, B.A. Conventional and Modern Techniques for Bioactive Compounds Recovery from Plants: Review. *Sci. Afr.* **2025**, *27*, e02509. [CrossRef]
12. Sanjai, C.; Gaonkar, S.L.; Hakkimane, S.S. Harnessing Nature's Toolbox: Naturally Derived Bioactive Compounds in Nanotechnology Enhanced Formulations. *ACS Omega* **2024**, *9*, 43302–43318. [CrossRef]
13. Atanasov, A.G.; Waltenberger, B.; Pferschy-Wenzig, E.-M.; Linder, T.; Wawrosch, C.; Uhrin, P.; Temml, V.; Wang, L.; Schwaiger, S.; Heiss, E.H.; et al. Discovery and Resupply of Pharmacologically Active Plant-Derived Natural Products: A Review. *Biotechnol. Adv.* **2015**, *33*, 1582–1614. [CrossRef] [PubMed]
14. Kundu, B.; Reis, R.L.; Kundu, S.C. Polysaccharides in Cancer Therapy. In *Polysaccharides of Microbial Origin: Biomedical Applications*; Springer: Berlin/Heidelberg, Germany, 2021; pp. 1–21.

15. Murphy, E.J.; Fehrenbach, G.W.; Abidin, I.Z.; Buckley, C.; Montgomery, T.; Pogue, R.; Murray, P.; Major, I.; Rezoagli, E.; Murphy, E.J.; et al. Polysaccharides—Naturally Occurring Immune Modulators. *Polymers* **2023**, *15*, 2373. [CrossRef] [PubMed]
16. Teixeira, S.; Ferreira, D.; Rodrigues, L.R.; Carvalho, M.A.; Castanheira, E.M.S.; Teixeira, S.; Ferreira, D.; Rodrigues, L.R.; Carvalho, M.A.; Castanheira, E.M.S. Albumin/Hyaluronic Acid Gel Nanoparticles Loaded with a Pyrimidine-Based Drug for Potent Anticancer Activity. *Gels* **2025**, *11*, 759. [CrossRef]
17. Khaing, E.M.; Intaraphairot, T.; Mahadlek, J.; Okonogi, S.; Pichayakorn, W.; Phaechamud, T.; Khaing, E.M.; Intaraphairot, T.; Mahadlek, J.; Okonogi, S.; et al. Imatinib Mesylate-Loaded Rosin/Cinnamon Oil-Based In Situ Forming Gel against Colorectal Cancer Cells. *Gels* **2022**, *8*, 526. [CrossRef]
18. Mohamed, S.A.; Elsherbini, A.M.; Alrefaey, H.R.; Adelrahman, K.; Moustafa, A.; Egodawaththa, N.M.; Crawford, K.E.; Nesnas, N.; Sabra, S.A.; Mohamed, S.A.; et al. Gum Arabic: A Commodity with Versatile Formulations and Applications. *Nanomaterials* **2025**, *15*, 290. [CrossRef]
19. Ahmed, A.A. Health Benefits of Gum Arabic and Medical Use. In *Gum Arabic: Structure, Properties, Application and Economics*; Academic Press: Cambridge, MA, USA, 2018; pp. 183–210.
20. Kamal, E.; Kaddam, L.A.; Dahawi, M.; Osman, M.; Salih, M.A.; Alagib, A.; Saeed, A. Gum Arabic Fibers Decreased Inflammatory Markers and Disease Severity Score among Rheumatoid Arthritis Patients, Phase II Trial. *Int. J. Rheumatol.* **2018**, *2018*, 4197537. [CrossRef]
21. Al-Jubori, Y.; Ahmed, N.T.B.; Albusaidi, R.; Madden, J.; Das, S.; Sirasanagandla, S.R.; Al-Jubori, Y.; Ahmed, N.T.B.; Albusaidi, R.; Madden, J.; et al. The Efficacy of Gum Arabic in Managing Diseases: A Systematic Review of Evidence-Based Clinical Trials. *Biomolecules* **2023**, *13*, 138. [CrossRef]
22. Ali, N.E.; Kaddam, L.A.; Alkarib, S.Y.; Kaballo, B.G.; Khalid, S.A.; Higawee, A.; AbdElhabib, A.; AlaaAldeen, A.; Phillips, A.O.; Saeed, A.M. Gum Arabic (*Acacia senegal*) Augmented Total Antioxidant Capacity and Reduced C-Reactive Protein among Haemodialysis Patients in Phase II Trial. *Int. J. Nephrol.* **2020**, *2020*, 7214673. [CrossRef]
23. Elnour, A.A.M.; Abdurahman, N.H.; Musa, K.H.; Rasheed, Z. Prebiotic Potential of Gum Arabic for Gut Health. *Int. J. Health Sci.* **2023**, *17*, 4–5.
24. Elnour, A.A.M.; Mirghani, M.E.S.; Kabbashi, N.A.; Md Alam, Z.; Musa, K.H. Study of Antioxidant and Anti-Inflammatory Crude Methanol Extract and Fractions of *Acacia seyal* Gum. *Am. J. Pharmacol. Pharmacother.* **2018**, *5*, 3. [CrossRef]
25. Obaid, S.S. The Medical Uses of Gum *Acacia*-Gum Arabic (GA) In Human. *Acad. J. Res. Sci. Publ.* **2020**, *1*, 1–11.
26. Hussein AlYafii, S.Y. Molecular Mechanisims Underlying the Anti-Cancer Activity of Gum Arabic from *Acacia* sp. in Triple-Negative Breast Cancer Cells. Master's Thesis, United Arab Emirates University, Al Ain, United Arab Emirates, 2021.
27. Pandit, A.H.; Mazumdar, N.; Imtiyaz, K.; Alam Rizvi, M.M.; Ahmad, S. Self-healing and injectable hydrogels for anticancer drug delivery: A study with multialdehyde gum arabic and succinic anhydride chitosan. *ACS Appl. Bio Mater.* **2020**, *3*, 8460–8470. [CrossRef]
28. Bashiri, G.; Shojaosadati, S.A.; Abdollahi, M. Synthesis and characterization of Schiff base containing bovine serum albumin-gum arabic aldehyde hybrid nanogels via inverse miniemulsion for delivery of anticancer drug. *Int. J. Biol. Macromol.* **2021**, *170*, 222–231. [CrossRef]
29. Venkatesan, J.; Hur, W.; Gupta, P.K.; Son, S.E.; Lee, H.B.; Lee, S.J.; Ha, C.H.; Cheon, S.H.; Kim, D.H.; Seong, G.H. Gum Arabic-mediated liquid exfoliation of transition metal dichalcogenides as photothermic anti-breast cancer candidates. *Int. J. Biol. Macromol.* **2023**, *244*, 124982. [CrossRef]
30. Sarika, P.R.; Nirmala, R.J. Curcumin loaded gum arabic aldehyde-gelatin nanogels for breast cancer therapy. *Mater. Sci. Eng. C* **2016**, *65*, 331–337. [CrossRef] [PubMed]
31. Soans, S.H.; Chonche, M.J.; Sharan, K.; Srinivasan, A.; Archer, A.C. Apoptotic and anti-inflammatory effect of nisin loaded sodium alginate-gum arabic nanoparticles against colon cancer cells. *Int. J. Biol. Macromol.* **2025**, *305*, 141747. [CrossRef]
32. Hassani, A.; Azarian, M.M.S.; Ibrahim, W.N.; Hussain, S.A. Preparation, characterization and therapeutic properties of gum arabic-stabilized gallic acid nanoparticles. *Sci. Rep.* **2020**, *10*, 17808. [CrossRef] [PubMed]
33. Hassani, A.; Mahmood, S.; Enezei, H.H.; Hussain, S.A.; Hamad, H.A.; Aldoghachi, A.F.; Hagar, A.; Doolaanea, A.A.; Ibrahim, W.N. Formulation, characterization and biological activity screening of sodium alginate-gum arabic nanoparticles loaded with curcumin. *Molecules* **2020**, *25*, 2244. [CrossRef] [PubMed]
34. Munot, N.; Kandekar, U.; Rikame, C.; Patil, A.; Sengupta, P.; Urooj, S.; Bilal, A. Improved mucoadhesion, permeation and in vitro anticancer potential of synthesized thiolated acacia and karaya gum combination: A systematic study. *Molecules* **2022**, *27*, 6829. [CrossRef]
35. Azeem, M.; Siddique, M.H.; Imran, M.; Zubair, M.; Mumtaz, R.; Younas, M.; Abdel-Maksoud, M.A.; El-Tayeb, M.A.; Rizwan, M.; Yong, J.W.H. Assessing anticancer, antidiabetic, and antioxidant capacities in green-synthesized zinc oxide nanoparticles and solvent-based plant extracts. *Heliyon* **2024**, *10*, e31456. [CrossRef]

36. Hashem, A.H.; Abdel-Maksoud, M.A.; Fatima, S.; Almutairi, S.M.; Ghorab, M.A.; El-Batal, A.I.; El-Sayyad, G.S. Synthesis and characterization of innovative GA@ Ag-CuO nanocomposite with potent antimicrobial and anti-cancer properties. *Sci. Rep.* **2025**, *15*, 689. [CrossRef]
37. Thipe, V.C.; Jatar, A.; Raphael Karikachery, A.; Katti, K.K.; Katti, K.V. Green nanotechnology of *Yucca filamentosa*-phytochemicals-functionalized gold nanoparticles—Antitumor efficacy against prostate and breast cancers. *Nanotechnol. Sci. Appl.* **2023**, *19*, 1–40. [CrossRef]
38. Akhtar, S.; Zuhair, F.; Nawaz, M.; Khan, F.A. Green synthesis, characterization, morphological diversity, and colorectal cancer cytotoxicity of gold nanoparticles. *RSC Adv.* **2024**, *14*, 36576–36592. [CrossRef]
39. Murugan, S.S.; Hur, W.; Son, S.E.; Lee, H.B.; Ha, C.H.; Lee, S.J.; Cheon, S.H.; Kim, D.H.; Jeon, S.M.; Choi, D.Y.; et al. The therapeutic efficacy of silver loaded rhenium disulfide nanoparticles as a photothermal agent for cancer eradication. *J. Photochem. Photobiol. B Biol.* **2024**, *250*, 112831. [CrossRef] [PubMed]
40. Al-Duais, M.A.; El Rabey, H.A.; Mohammed, G.M.; Al-Awthan, Y.S.; Althiyabi, A.S.; Attia, E.S.; Rezk, S.M.; Tayel, A.A. The anticancer activity of fucoidan coated selenium nanoparticles and curcumin nanoparticles against colorectal cancer lines. *Sci. Rep.* **2025**, *15*, 287. [CrossRef] [PubMed]
41. Shahein, S.A.; Aboul-Enein, A.M.; Higazy, I.M.; Abou-Elella, F.; Lojkowski, W.; Ahmed, E.R.; Mousa, S.A.; AbouAitah, K. Targeted anticancer potential against glioma cells of thymoquinone delivered by mesoporous silica core-shell nanoformulations with pH-dependent release. *Int. J. Nanomed.* **2019**, *14*, 5503–5526. [CrossRef] [PubMed]
42. Alahmadi, N.; Hussein, M.A. Impact of Ag/ZnO reinforcements on the anticancer and biological performances of CA@ Ag/ZnO nanocomposite materials. *Molecules* **2023**, *28*, 1290. [CrossRef]
43. Jayalakshmi, C.S.; Haider, M.; Sanpui, P. Tyrosine kinase inhibitor-loaded zein nanoparticles with enhanced drug delivery and anticancer efficacy. *Int. J. Biol. Macromol.* **2025**, *314*, 143898. [CrossRef]
44. AbouAitah, K.; Stefanek, A.; Higazy, I.M.; Janczewska, M.; Swiderska-Sroda, A.; Chodara, A.; Wojnarowicz, J.; Szałaj, U.; Shahein, S.A.; Aboul-Enein, A.M.; et al. Effective targeting of colon cancer cells with piperine natural anticancer prodrug using functionalized clusters of hydroxyapatite nanoparticles. *Pharmaceutics* **2020**, *12*, 70. [CrossRef]
45. El-Sayyad, G.S.; El-Sayed, E.S.R.; Rizk, S.H.; Abdel-Maksoud, M.A.; Zakri, A.M.; Malik, A.; Malash, M.N.; Hashem, A.H. An eco-friendly and cost-effective approach for the synthesis of a novel GA@ CuO–ZnO nanocomposite: Characterization, antimicrobial and anticancer activities. *RSC Adv.* **2025**, *15*, 513–523. [CrossRef] [PubMed]
46. Thipe, V.C.; Panjtan Amiri, K.; Bloebaum, P.; Raphael Karikachery, A.; Khoobchandani, M.; Katti, K.K.; Jurisson, S.S.; Katti, K.V. Development of resveratrol-conjugated gold nanoparticles: Interrelationship of increased resveratrol corona on anti-tumor efficacy against breast, pancreatic and prostate cancers. *Int. J. Nanomed.* **2019**, *14*, 4413–4428. [CrossRef]
47. Namasivayam, S.K.R.; Rabel, A.M.; Prasana, R.; Bharani, R.A.; Nachiyar, C.V. Gum acacia PEG iron oxide nanocomposite (GA-PEG-IONC) induced pharmacotherapeutic activity on the Las R gene expression of *Pseudomonas aeruginosa* and HOXB13 expression of prostate cancer (PC3) cell line: A green therapeutic approach of molecular mechanism inhibition. *Int. J. Biol. Macromol.* **2021**, *190*, 940–959. [CrossRef] [PubMed]
48. Brown, W.; Marques, M. USP and Dissolution—20 Years of Progress. *Dissolut. Technol.* **2014**, *21*, 24–27. [CrossRef]
49. US Pharmacopeia (USP). Available online: https://www.usp.org/ (accessed on 23 December 2025).
50. Gökçe, H.B.; Aslan, İ. Novel Liposome–Gel Formulations Containing a Next Generation Postbiotic: Characterization, Rheological, Stability, Release Kinetic, and In Vitro Antimicrobial Activity Studies. *Gels* **2024**, *10*, 746. [CrossRef]
51. Kurt, A.A.; Ibrahim, B.; Çınar, H.; Atsü, A.N.; Bursalıoğlu, E.O.; Bayır, İ.; Özmen, Ö.; Aslan, İ. Nanoemulsion Hydrogel Delivery System of *Hypericum perforatum* L.: In Silico Design, In Vitro Antimicrobial–Toxicological Profiling, and In Vivo Wound-Healing Evaluation. *Gels* **2025**, *11*, 431. [CrossRef]
52. Kurt, A.A.; Aslan, İ. A Novel Liposomal In-Situ Hydrogel Formulation of *Hypericum perforatum* L.: In Vitro Characterization and In Vivo Wound Healing Studies. *Gels* **2025**, *11*, 165. [CrossRef]
53. Kaddam, L.; FdleAlmula, I.; Eisawi, O.A.; Abdelrazig, H.A.; Elnimeiri, M.; Lang, F.; Saeed, A.M. Gum Arabic as Fetal Hemoglobin Inducing Agent in Sickle Cell Anemia; in Vivo Study. *BMC Hematol.* **2015**, *15*, 19. [CrossRef]
54. Alobaidi, S. Therapeutic Potential of Gum Arabic (*Acacia senegal*) in Chronic Kidney Disease Management: A Narrative Review. *J. Clin. Med.* **2024**, *13*, 5778. [CrossRef]
55. Verbeken, D.; Dierckx, S.; Dewettinck, K. Exudate Gums: Occurrence, Production, and Applications. *Appl. Microbiol. Biotechnol.* **2003**, *63*, 10–21. [CrossRef] [PubMed]
56. Ali, B.H.; Ziada, A.; Blunden, G. Biological Effects of Gum Arabic: A Review of Some Recent Research. *Food Chem. Toxicol.* **2009**, *47*, 1–8. [CrossRef]
57. Babiker, R.; Merghani, T.H.; Elmusharaf, K.; Badi, R.M.; Lang, F.; Saeed, A.M. Effects of Gum Arabic Ingestion on Body Mass Index and Body Fat Percentage in Healthy Adult Females: Two-Arm Randomized, Placebo Controlled, Double-Blind Trial. *Nutr. J.* **2012**, *11*, 111. [CrossRef]

58. Mirghani, M.; Elnour, A.; Kabbashi, N.; Alam, Z.; Musa, K.H.; Abdullah, A. Determination of Antioxidant Activity of Gum Arabic: An Exudation from Two Different Locat; ions. *ScienceAsia* **2018**, *44*, 179–186. [CrossRef]
59. Baien, S.H.; Seele, J.; Henneck, T.; Freibrodt, C.; Szura, G.; Moubasher, H.; Nau, R.; Brogden, G.; Mörgelin, M.; Singh, M. Antimicrobial and Immunomodulatory Effect of Gum Arabic on Human and Bovine Granulocytes against Staphylococcus Aureus and *Escherichia coli*. *Front. Immunol.* **2020**, *10*, 3119. [CrossRef]
60. Babiker, R.; Kaddam, L.; Mariod, A. The Role of Gum Arabic as an Anti-Inflammatory, Antioxidant, and Immune Modulator in COVID-19: A Review. *Funct. Food Sci.* **2022**, *2*, 242–257. [CrossRef]
61. Fadaka, A.O.; Meyer, S.; Ahmed, O.; Geerts, G.; Madiehe, M.A.; Meyer, M.; Sibuyi, N.R.S.; Fadaka, A.O.; Meyer, S.; Ahmed, O.; et al. Broad Spectrum Anti-Bacterial Activity and Non-Selective Toxicity of Gum Arabic Silver Nanoparticles. *Int. J. Mol. Sci.* **2022**, *23*, 1799. [CrossRef] [PubMed]
62. Ma, T.; Du, J.; Zhang, Y.; Wang, Y.; Wang, B.; Zhang, T. GPX4-Independent Ferroptosis—A New Strategy in Disease's Therapy. *Cell Death Discov.* **2022**, *8*, 434. [CrossRef] [PubMed]
63. Wei, L.; Feng, Z.; Dou, Q.; Mao, G.; Zhao, H.; Zhao, X.; Hao, B. GSTA2 Overexpression Alleviates Bis (2-Ethylhexyl) Phthalate (DEHP)-Induced Male Reproductive Disorders by Inhibiting Oxidative Stress-Mediated Cell Apoptosis via the Activated PI3K/AKT Signaling Pathway. *Mol. Cell. Endocrinol.* **2025**, *599*, 112462. [CrossRef]
64. Lingappan, K. NF-κB in Oxidative Stress. *Curr. Opin. Toxicol.* **2018**, *7*, 81–86. [CrossRef]
65. Stockwell, B.R.; Angeli, J.P.F.; Bayir, H.; Bush, A.I.; Conrad, M.; Dixon, S.J.; Fulda, S.; Gascón, S.; Hatzios, S.K.; Kagan, V.E.; et al. Ferroptosis: A Regulated Cell Death Nexus Linking Metabolism, Redox Biology, and Disease. *Cell* **2017**, *171*, 273–285. [CrossRef] [PubMed]
66. Karbakhsh Ravari, F.; Ghasemi Gorji, M.; Rafiei, A. From Iron-Driven Cell Death to Clot Formation: The Emerging Role of Ferroptosis in Thrombogenesis. *Biomed. Pharmacother.* **2025**, *189*, 118328. [CrossRef] [PubMed]
67. Ighodaro, O.M.; Akinloye, O.A. First Line Defence Antioxidants-Superoxide Dismutase (SOD), Catalase (CAT) and Glutathione Peroxidase (GPX): Their Fundamental Role in the Entire Antioxidant Defence Grid. *Alex. J. Med.* **2018**, *54*, 287–293. [CrossRef]
68. *ISO 3219-2:2021*; Rheology—Part 2: General Principles of Rotational and Oscillatory Rheometry. International Organization for Standardization: Geneva, Switzerland, 2021.
69. *ASTM D2196-18*; Standard Test Methods for Rheological Properties of Non-Newtonian Materials by Rotational Viscountess. ASTM: West Conshohocken, PA, USA, 2018.
70. Barnes, H.A.; Hutton, J.F.; Walters, K. *An Introduction to Rheology*; Elsevier: Amsterdam, The Netherlands, 1989; Volume 3.